Nucleic Acid Interactions of Unfused Aromatic Cations: Evaluation of Proposed Minor-Groove, Major-Groove, and Intercalation Binding Modes

W. David Wilson,*,† Farial A. Tanious,† Daoyuan Ding,† Arvind Kumar,† David W. Boykin,*,† Pierre Colson,‡ Claude Houssier,‡ and Christian Bailly*,§

Contribution from the Department of Chemistry, Georgia State University, Atlanta, Georgia 30303; INSERM U-124 et Laboratoire de Pharmacologie Antitumorale du Centre Oscar Lambret, IRCL, Place de Verdun, 59045 Lille, France; and Laboratoire de Chimie Macromoléculaire et Chimie Physique, Université de Liège, Liège 4000, Belgium

Received April 10, 1998

Abstract: Amidine derivatives of the 2,5-diphenylfuran aromatic system have activity against a variety of microorganisms. The compounds bind strongly to continuous sequences of AT base pairs in DNA, and there is general agreement that the compounds complex in the minor groove in AT sequences. Some of the derivatives also bind strongly in GC rich and mixed sequences of DNA, and both major-groove and intercalation binding modes have been suggested for this binding mode on the basis of different experimental observations. To obtain definitive information on the DNA binding modes of these types of compounds, we have synthesized additional derivatives, which were designed to provide improved distinction between major-groove and intercalation binding modes, and have extended the experimental analysis to include electric linear dichroism, high-resolution NMR, and absorption, fluorescence, and CD spectroscopy results. All of the spectral results as well as kinetics studies results support a minor-groove binding mode in AT sequences of DNA, as expected, while results with sequences containing GC or mixed AT and GC sequences support an intercalation mode for these compounds. The weak induced CD signals for the compounds in complex with poly $d(G-C)_2$, for example, are characteristic of intercalation and the electric linear dichroism spectra demonstrate clearly that the compounds have their transition dipoles oriented in the same plane as the DNA base pairs, exactly as predicted for intercalation binding. Chemical shift changes of the aromatic proton signals of the diphenylfuran ring system are all upfield by approximately 0.5 ppm or greater on complex formation with GC sequences, also as predicted for intercalation. The compounds have NOE contacts to DNA protons in both the major and the minor grooves, and this is only possible if the compounds extend through the DNA double helix, as expected for an intercalation binding mode. Some of the discrepancy in the literature may have arisen due to confusion caused by the mixed minor-groove and intercalation complexes of the diphenylfurans in heterogeneous sequence DNA.

Introduction

Unfused aromatic cations related to furamidine (DB 75) and furimidazoline (DB 60) (Figure 1) have shown very promising biological activity against a variety of microorganisms.[1−6] Alkyl derivatives of furamidine have shown particularly good activity against opportunistic infections such as *Pneumocystis carinii* (*P. carinii*), the organism that is the leading cause of death in AIDS patients. The biological activity is strongly dependent on substituent structure. The cyclopentyl derivative (DB 244) in Figure 1, for example, is one of the most active compounds in this series, while the closely related 3-pentyl compound (DB 226) is approximately 250-fold less active.[4] The compounds are related in structure to pentamidine, and, as with pentamidine and analogues, their antimicrobial activity is correlated with their ability to interact strongly with the DNA minor groove in AT sequences with subsequent inhibition of one or more DNA directed enzymes.[7,8] Compounds in this series have also demonstrated significant biological activity in human tumor cell lines resistant to cisplatinum, and the activity correlates with their DNA binding affinity.[9]

Studies of a variety of unfused aromatic cations, which do

* Address correspondence to any of these authors.
† Georgia State University.
§ COL-INSERM U124.
‡ Université de Liège.

(1) Das, B. P.; Boykin, D. W. *J. Med. Chem.* **1977**, *20*, 531−536.
(2) Boykin, D. W.; Kumar, A.; Spychala, J.; Zhou, M.; Lombardy, R. J.; Wilson, W. D.; Dykstra, C. C.; Jones, S. K.; Hall, J. E.; Tidwell, R. R.; Laughton, C.; Nunn, C. M.; Neidle, S. *J. Med. Chem.* **1995**, *38*, 912−916.
(3) Trent, J. O.; Clark, G. R.; Neidle, S.; Kumar, A.; Wilson, W. D.; Boykin, D. W.; Hall, J. E.; Tidwell, R. R.; Blackburn, B. L. *J. Med. Chem.* **1996**, *39*, 4554−4562.
(4) Boykin, D. W.; Kumar, A.; Xiao, G.; Wilson, W. D.; Bender, B. K.; McCurdy, D. R.; Hall, J. E.; Tidwell, R. R. *J. Med. Chem.* **1998**, *41*, 123−129.
(5) Del Poeta, M.; Schell, W. A.; Dykstra, C. C.; Jones, S.; Tidwell, R. R.; Kumar, A.; Boykin, D. W.; Perfect, J. R. In press.
(6) Hopkins, K. T.; Wilson, W. D.; Bender, B. K.; McCurdy, D. R.; Hall, J. E.; Tidwell, R. R.; Kumar, A.; Bajic, M.; Boykin, D. W. In press.
(7) Bell, C. A.; Dykstra, C. C.; Naiman, N. N.; Cory, M.; Fairly, T. A.; Tidwell, R. R. *Antimicrob. Agents Chemother.* **1993**, *37*, 2668−2673.
(8) Hildebrant, E.; Boykin, D. W.; Kumar, A.; Tidwell, R. R.; Dykstra, C. C. *J. Eur. Microbiol.* **1998**, *45*, 112−121.
(9) Neidle, S.; Kelland, L. R.; Trent, J. O.; Simpson, I. J.; Boykin, D. W.; Kumar, A.; Wilson, W. D. *Biorg. Med. Chem. Lett.* **1997**, *7*, 1403−1408.

S0002-7863(98)01212-8 CCC: $15.00
Published on Web 09/29/1998

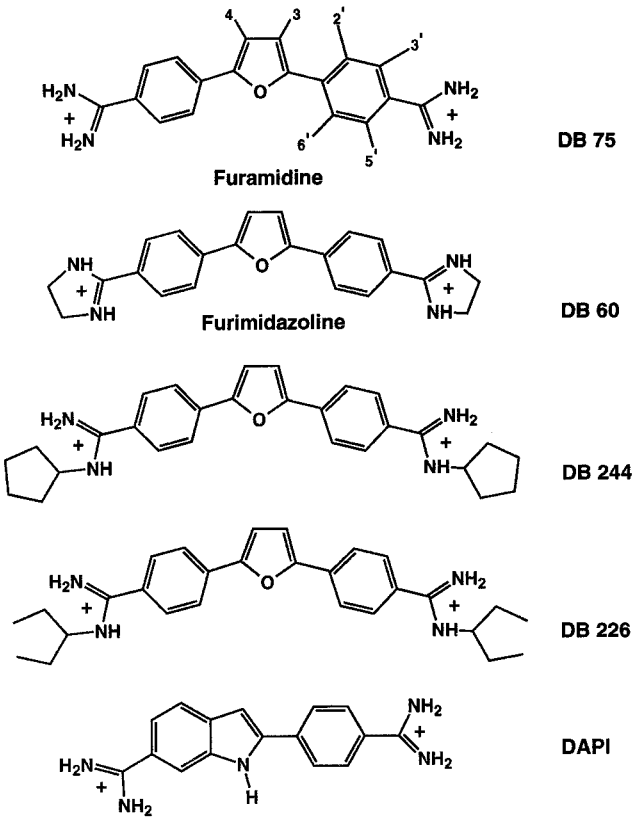

Figure 1. Structure of the furan derivatives used in this research and DAPI.

not have the phenylamidine groups of the compounds of Figure 1, indicated that such unfused aromatic systems bind to DNA by intercalation, not by a minor-groove mode.[10−13] In addition, conversion of the phenylamidine groups of (DB 75) to benzylamine groups converts the compound into an intercalator at both GC and AT sites.[14] These observations raised the question of whether amidine derivatives that bind in the minor groove at AT sequences could also bind to GC and mixed GC/AT sequences, and if so, how strongly and by what mode do they bind? Our initial results were quite surprising. Some compounds related to those shown in Figure 1 can bind in GC sequences as strongly as classical intercalators such as ethidium.[14−17] We also found that the GC binding depended strongly on the aromatic ring system of the compounds being able to assume a relatively planar conformation. Compounds such as netropsin and pentamidine which do not have an extended aromatic system bind strongly to AT sites but very weakly in GC sequences of DNA and to RNA.[18,19] The GC interactions of the nonplanar compounds is probably through a weak complex with the DNA anionic backbone.

A detailed series of studies on the well-characterized compound, DAPI (Figure 1), which is similar in structure to the diphenylfurans and is known to bind strongly in the minor groove at AT sequences, indicated that it also bound to GC sites.[20−22] NMR, hydrodynamic, kinetics, modeling,[20,21] and electric linear dichroism [22] studies strongly suggested that the binding mode for the unfused aromatic system of DAPI in GC sequences in DNA and in RNA was by intercalation. Similar detailed studies with berenil, a related diamidine, also indicated that it could bind by both minor-groove and intercalation modes.[23,24] As with berenil, DAPI intercalated into polyd(G−C)$_2$ and polyrA·polyrU as well as other DNA duplexes[20−22] and into the triplex structure composed of two polydT and one polyrA strand.[25] As noted above, our preliminary analysis of GC complexes of the furan DB 75 also suggested an intercalation binding mode;[14] however, studies by other investigators with heterogeneous natural sequence DNAs by flow linear dichroism[26] and by atomic force microscopy[27] and with poly d(G−C)$_2$ by flow dichroism[26] yielded results that were interpreted in terms of a nonintercalation binding mode for DB 75 in all DNA sequences. A major-groove binding mode for DB 75 was suggested on the basis of the flow dichroism studies.[26]

Although there are a large number of well-characterized AT specific compounds that bind to DNA in the minor groove,[28] designing compounds to recognize GC sequences has been more challenging, and there has been little success in targeting the major groove with strong binding agents for any sequence.[13] To understand the array of GC specific recognition modes in more detail, it is essential to clearly establish the binding mode of DB 75 and other related derivatives to GC sequences in DNA; do these compounds intercalate or do they provide us with a new lead into major-groove recognition modes? In addition, it is essential to understand the complete set of interactions that these compounds have with DNA in order to understand the significance of the GC interactions to their activity as antimicrobial agents.[1−6] To obtain definitive information on the DNA binding modes of these types of compounds, we have synthesized additional derivatives (Figure 1) and extended the analysis to include electric linear dichroism methods with a variety of different sequences of DNA and high-resolution NMR methods with different lengths and sequences of DNA as well as absorption, fluorescence, and circular dichroism (CD) spectros-

(10) Wilson, W. D.; Strekowski, L.; Tanious, F.; Watson, R.; Mokrosz, J. L.; Strekowska, A.; Webster, G.; Neidle, S. *J. Am. Chem. Soc*. **1988**, *110*, 8292−8299.

(11) Wilson, W. D.; Tanious, F. A.; Watson, R. A.; Barton, H. J.; Strekowska, A.; Harden, D. B.; Strekowski, L. *Biochemistry* **1989**, *28*, 1984−1992.

(12) Wilson, W. D.; Barton, H. J.; Tanious, F. A.; Kong, S. B.; Strekowski, L. *Biophys. Chem*. **1990**, *35*, 227−243.

(13) Wilson, W. D. In *Nucleic Acids in Chemistry and Biology*, 2nd ed.; Blackburn, G. M., Gait, M. J., Eds.; IRL Press: Oxford, U.K., 1996; Chapter 8.

(14) Wilson, W. D.; Tanious, F. A.; Buczak, H.; Venkatramanan, M. K.; Das, B. P.; Boykin, D. W. In *Molecular Basis of Specificity in Nucleic Acid-Drug Interactions*; Pullman, B., Jortner, J., Eds.; Kluwer Academic Publishers: Dordrecht, The Netherlands, 1990; pp 331−353.

(15) Wilson, W. D.; Tanious, F. A.; Buczak, H.; Ratmeyer, L.; Venkatramanan, M. K.; Kumar, A.; Boykin, D. W.; Munson, R. In *Structure and Function: Nucleic Acids*; Sarma, R. H., Sarma, M. H., Eds.; Adenine Press: Schenectady, NY, 1992; Vol. I, pp 83−105.

(16) Tanious, F. A.; Spychala, J.; Kumar, A.; Greene, K.; Boykin, D. W.; Wilson, W. D. *J. Biomol. Struct. Dyn.* **1994**, *11*, 1063−1083.

(17) Wilson, W. D.; Tanious, F. A.; Barton, H. J.; Wydra, R. L.; Jones, R. L.; Boykin, D. W.; Strekowski, L. *Anti-Cancer Drug Des.* **1990**, *5*, 31−42.

(18) Zimmer, C.; Wahnert, U. *Prog. Biophys. Mol. Biol*. **1986**, *47*, 31−112.

(19) Wilson, W. D.; Ratmeyer, L.; Zhao, M.; Strekowski, L.; Boykin, D. W. *Biochemistry* **1993**, *32*, 4098−4104.

(20) Wilson, W. D.; Tanious, F.; Barton, H.; Jones, R.; Strekowski, L.; Boykin, D. *J. Am. Chem. Soc.* **1989**, *111*, 5008−5010.

(21) Wilson, W. D.; Tanious, F. A.; Barton, H. J.; Jones, R. L.; Fox, K.; Wydra, R. L.; Strekowski, L. *Biochemistry* **1990**, *29*, 8452−8461.

(22) Colson, P.; Houssier, C.; Bailly, C. *J. Biomol. Struct. Dyn.* **1995**, *13*, 351−366.

(23) Pilch, D. S.; Kirolos, M. A.; Liu, X.; Plum, G. E.; Breslauer, K. J. *Biochemistry* **1995**, *34*, 9962−9976.

(24) Pilch, D. S.; Kirolos, M. A.; Breslauer, K. J. *Biochemistry* **1995**, *34*, 16107−16124.

(25) Xu, Z.; Pilch, D. S.; Srinivasan, A. R.; Olson, W. K.; Geacintov, N. E.; Breslauer, K. J. *Bioorg. Med. Chem.* **1997**, *5*, 1137−1147.

(26) Jansen, K.; Lincoln, P.; Norden, B. *Biochemistry* **1993**, *32*, 6605−6612.

(27) Coury, J. E.; McFail-Isom, L.; Williams, L. D.; Bottomley, L. A. *Proc. Natl. Acad. Sci. U.S.A.* **1996**, *93*, 12283−12286.

(28) Bailly, C. In *Advances in DNA Sequence Specific Agents*; Palumbo, M.; Ed.; JAI Press Inc.: Greenwich, CT, 1998; Vol. 3, pp 97−156.

copy. Although several X-ray structures of furan derivatives in the minor groove in AT sequences have been determined,[3,29] no high-resolution structure is available for the GC binding mode, and structural information is essential for our understanding of the differences in molecular recognition of small aromatic cations by AT and GC rich sequences of DNA. Starting with furamidine (DB 75), the design of the compounds in Figure 1 was directed toward distinguishing minor-groove, major-groove, and intercalation binding modes. Furimidazoline, DB 60, is predicted by ab initio calculations to have a relatively flat structure, whereas the calculations predicted a significant twist for all amidine derivatives. DB 60 should then bind better to intercalation sites, while DB 75 should fit as well or better into the helical twist of the minor groove in AT sequences. The alkyl derivatives were designed to prove possible major groove binding. The cyclopentyl derivative DB 244 should be able to fit into the minor groove while the narrow groove width should hinder binding of DB 226. If the major groove is the binding site for these compounds in GC sequences, however, DB 226 should be able to interact quite well in that wider groove and could be the strongest binding compound in GC sequences. The conclusion from all of the studies reported here is that unfused aromatic cations, such as those shown in Figure 1, bind in the minor groove in AT sequences, but bind by intercalation in GC and mixed sequence regions of DNA. We also provide an explanation of how incorrect conclusions about the DNA binding modes of such compounds can be reached from analyses with heterogeneous linear DNA.

Experimental Section

Compounds. The furan compounds were prepared as reported previously.[1−6] Purity of all compounds was verified by NMR and elemental analysis.

Buffers. MES (2-(*N*-morpholino)ethanesulfonic acid) buffer contained 0.01 M MES and 10^{-3} M ethylenediaminetetraacetic acid (EDTA). Sodium chloride was added to adjust the ionic strength, and the pH was adjusted to 6.2 with NaOH. Phosphate buffer contained 7.5 mM sodium phosphate, 100 mM NaCl, and 0.01 mM EDTA, pH 7.0. For electric linear dichroism (ELD) experiments all nucleic acids were dialyzed against 1 mM sodium cacodylate buffer, pH 6.5.

DNA. All double-stranded polynucleotides were purchased from Pharmacia and were prepared as previously described.[22,30] Calf thymus DNA (CT-DNA, Sigma) was deproteinized with sodium dodecyl sulfate (protein content < 0.2%) prior to use. The polymer concentrations were determined by applying molar extinction coefficients given in the literature.[31] The oligomers d(G−C)$_7$, d(GCGC), d(CGCG), d(ACGT), d(CGCGAATTCGCG), and d(GCGAATTCGC) (Midland Certified Reagent Co.) and were purified by HPLC and desalted. Purity was checked by NMR. The concentrations were determined optically using extinction coefficients per mole of strand at 260 nm determined by the nearest neighbor procedure.[32]

Absorption Spectroscopy. UV−vis scans were obtained with a Cary 4 spectrophotometer in MES with 0.1 M NaCl added. Spectrophotometric binding measurements have been described.[30]

Fluorescence Spectroscopy. Fluorescence spectra were obtain using a Photon Technology International (PTI) spectrometer with Felix software to control the instrument and collect the fluorescence data. Typically, the fluorescence intensity for the compound was measured at 20 °C in MES buffer, the samples were excited at 358 nm for DB 226 and DB 244 and at 360 nm for DB 60, and the fluorescence emission was monitored. The solution of the compound was titrated with aliquots of DNA stock solution. The following equation were used to calculate C_b, the concentration of bound compound:

$$C_b = (I_0 - I_i)/[(1 - I_b/I_0)(I_0/C_0)] \quad (1)$$

where I_0 is the initial fluorescence intensity, I_i is the fluorescence intensity at each concentration of DNA, I_b is the fluorescence intensity at saturation, and C_0 is the initial concentration of the compound. The concentration of the free compound and the Scatchard parameters can be obtained from

$$C_{free} = C_0 - C_b \quad (2)$$

Circular Dichroism. CD spectra were obtained on a Jasco J-710 spectrometer interfaced to an IBM-PC computer. The software supplied by Jasco provided instrument control and data acquisition. Solutions of the compounds in MES buffer at 25 °C were scanned in 1 cm quartz cuvettes to examine if the compound has CD. A solution of the DNA was scanned, the compound then added, and the sample rescanned at all desired ratios.

Kinetics. Kinetics experiments were conducted on an Olis RSM 1000 scanning stopped-flow spectrometer interfaced to a Gateway 2000 PC computer. Data collection and analysis were with the RSM-1000 software. Single exponential fits to the results generally give unsatisfactory residuals and significantly higher root mean square deviations with all the complexes of these compounds with polyd(A−T)$_2$ and polyd(G−C)$_2$. Two exponential fits to the data give satisfactory residuals, and three exponential fits do not significantly improve the residuals or root mean square deviations. For the purposes of comparison, the dissociation lifetime (τ) and apparent rate constant ($k_{app} = 1/\tau$) were calculated from the computer-derived, best-fit values for rate constants and amplitudes:

$$\tau = 1/(A_1k_1 + A_2k_2)$$

where A and k values refer to the amplitudes and rate constants for the two exponential fits to the dissociation results.[33]

Electric Linear Dichroism (ELD). ELD measurements were performed using a computerized optical measurement system built by Houssier.[34] The procedures outlined previously were followed.[34] The optical setup incorporating a high-sensitivity T-jump instrument equipped with a Glan polarizer was used under the following conditions: bandwidth, 3 μM; sensitivity limit, 0.001 in $\Delta A/A$; response time, 3.5 s. Equations used for the calculation of the different parameters have been reported.[35,36] All experiments were conducted at 20 °C with a 10 mm path length Kerr cell having 1.5 mm electrode separation, in 1 mM sodium cacodylate buffer, pH 6.5. The DNA samples were oriented under an electric field strength of 13 kV/cm, and the drug under test was present at 10 μM together with the DNA or polynucleotide at 100 μM unless otherwise stated. This electrooptical method has proved most useful as a means of determining the orientation of drugs bound to DNA and has the additional advantage that it senses only the orientation of the polymer-bound ligand: free ligand is isotropic and does not contribute to the signal.[36,37]

To investigate the geometry of drug binding to DNA by ELD, the reduced dichroism $\Delta A/A$ of a ligand−DNA complex measured in the ligand absorption band must be analyzed with respect to the reduced dichroism measured for the same DNA or polynucleotide at 260 nm in the absence of drug, $(\Delta A/A)^{DNA}$. The reduced dichroism ratio DR

(29) Laughton, C. A.; Tanious, F. A.; Nunn, C. M.; Boykin, D. W.; Wilson, W. D.; Neidle, S. *Biochemistry* **1996**, *35*, 5655−5661.
(30) Wilson, W. D.; Wang, Y.-H.; Kusuma, S.; Chandrasekaran, S.; Yang, N. C.; Boykin, D. W. *J. Am. Chem. Soc.* **1985**, *107*, 4989−4995.
(31) Wilson, W. D.; Tanious, F. A.; Fernandez-Sais, M.; Rigl, C. T. in *Drug−DNA Interaction Protocolols*; Fox, K. R., Ed.; Humana Press: Totowa, NJ, 1997; pp 219−240.
(32) Fasman, G. D. In *Nucleic Acids*; Fasman, G. D., Ed.; CRC Press: Cleveland, OH, 1975; p 589.
(33) Wilson, W. D.; Tanious, F. A. In *Molecular Aspects of Anticancer Drug−DNA Interactions*; Neidle S., Waring, M., Eds.; The Macmillan Press Ltd.: London, 1994; pp 243−269.
(34) Houssier, C.; O'RKonski, C. T. In *Molecular Electrooptics*; Krause, S., Ed.; Plenum Publishing Corp.: New York, 1981; pp 309−339.
(35) Houssier, C. In *Molecular Electrooptics*; Krause, S., Ed., Plenum Publishing Corp.: New York, 1981; pp 363−398.
(36) Bailly, C.; Hinichart, J. P.; Colson, P.; Houssier, C. *J. Mol. Recognit.* **1992**, *5*, 155−171.
(37) Colson, P.; Bailly, C.; Houssier, C. *Biophys. Chem.* **1996**, *58*, 125−140.

is defined as follows: DR = $[(\Delta A/A)^{\text{ligand-DNA}}]/[(\Delta A/A)^{\text{DNA}}]$. The numerator refers to the reduced dichroism of the drug−DNA complex measured at the absorption maximum of the ligand bound to DNA. The denominator is always negative under the experimental conditions used. The dichroism ratio is expected to be +1 if the transition moment of the drug chromophore is parallel to the DNA bases, as in the case of complete intercalative binding. For groove binders, the angle between the double helical axis and the long axis of the chromophore lies below 54° which gives rise to positive dichroism and thus to a negative DR value. Under these conditions, the reduced dichroism ratios for any given drug−DNA and drug−polynucleotide complexes can be mutually compared with good relative accuracy, independent of the polymer size.[36,37]

NMR Spectra. NMR spectra were obtained on a Varian Unity plus 600 spectrometer as previously described.[20,21,38] Data were processed either by Vnmr 5.1 software from Varian or with the program FELIX (Biosym Technologies, San Diego, CA). Typical conditions for the collection of spectra in D_2O included the following: 6000 Hz spectral width, 16000 complex data points, 200 scans, 2 s relaxation delay, 0.6 mL sample in a 5 mm NMR tube, and 1.0 Hz line broadening before Fourier transformation. All NMR spectra were obtained in phosphate buffer solution (7.5 mM NaH_2PO_4; 10^{-5} M EDTA, pH 7.0; 0.10 M NaCl). Samples were referenced to (2,2-dimethylsilapentane-5-sulfonate) DSS using the calibrated position of the water peak relative to DSS. Assignment of the aromatic proton signals for the drug−DNA complexes were made via drug−DNA titrations or melting 1D or 2D COSY experiments. The residual HDO peak was used as an internal reference. Two-dimensional experiments were obtained with a spectral width of 6000 Hz in both dimensions with 2048 complex data points in the t_2 dimension and 512 points in the t_1 dimension. Phase sensitive NOESY spectra were obtained with a mixing time of 300 ms using the method of States et al.[39]

Molecular Modeling. All models were built and energy minimized using the software package Sybyl (v6.03, Tripos). The Kollman all-atom force field[40,41] was used with minor modifications, as described previously.[42]

Results

Absorption and Fluorescence Emission Spectroscopy. The diphenylfuran amidine derivatives have strong absorption bands and fluorescence emission spectra in the visible and near UV spectral region. Full absorption spectra for all four furan derivatives of Figure 1 are shown in Figure S1 (Supporting Information). Both the absorption and the emission spectra are strongly perturbed when the furans form complexes with DNA. All four furan derivatives of Figure 1 have similar induced spectral changes on complex formation with poly$d(A-T)_2$ and similar changes on complex formation with poly$d(G-C)_2$. The changes induced by binding to the AT and GC polymers are, however, quite different (Figure 2). The same conclusion is reached from analysis of fluorescence changes on interactions of the compounds with AT and GC sites (Figure 2). The compounds do not have isoemmisive behavior in the titrations with poly$d(A-T)_2$ at high compound to DNA ratios (Figure 2E,G), but isoemmisive behavior is observed at lower compound concentrations. The loss of isoemmisive behavior at the higher compound concentrations and ratios suggests that a weaker secondary binding mode is observed under those conditions.

Quantitative analysis of the spectral results with the McGhee−von Hippel equation[43] allows a determination of the *K* value for the interactions. Determination of binding constants was done under conditions where isoemmisive behavior is observed in fluorescence titrations. Scatchard plots of the results for DB 60 at several ionic strengths are shown in Figure S2 (Supporting Information) along with best fit curves. The inset in the figure shows a linear plot of log K versus − log[Na^+] with a slope of 2.1 as expected for a dication binding to DNA. Other derivatives gave similar slopes. Table 1 contains binding results for all compounds with the AT and GC polymers under a fixed set of conditions. In general the binding constants for AT polymers are significantly higher than those observed for binding to the GC polymers.

Electric Linear Dichroism. The absorption bands of the compounds complexed to the different DNAs can be used to evaluate the orientations of the compound aromatic system (planar diphenylfuran) relative to the DNA base pairs by use of electric linear dichroism. In preliminary experiments, calf thymus DNA (which contains a roughly equal mixture of A·T and G·C base pairs) was used to determine the amount of drugs required to obtain full binding to DNA under the ELD conditions. The maximum reduced dichroism $\Delta A/A$ was obtained for DNA−drug ratio ≥ 10 (data not shown). This ratio of 10 was maintained for the subsequent ELD measurements. Reduced dichroism spectra for the furan derivatives complexed with CT DNA and several polynucleotides are compared in Figure 3. The ELD values at the compound absorption maxima are all positive for poly $d(A-T)_2$ and increase in the order DB 244 > DB 75 > DB 226 ≈ DB 60. With poly$d(G-C)_2$ the reduced dichroism values are all negative, as for DNA base pairs, and increase in the order DB 60 > DB 226 ≈ DB 244 > DB 75. ELD values for poly$d(I-C)_2$, which has base pairs similar to GC but without the G amino group in the minor groove, are similar to the AT values. The mixed sequence CT DNA has near zero ELD values for DB 75, DB 226, and DB 244, while the value for DB 60 is negative (Figure 4). Polymers with mixed AT and GC base pairs, i.e., poly(dA-dC)·(dG-dT) and poly(dA-dG)·(d(C-dT), also yield much more negative reduced dichroism values with DB 60 than with the other three diphenylfuran derivatives (Figure 3).

The ELD data are summarized in Figure 4, which shows the variation of the dichroism ratio DR (i.e. the reduced dichroism of the drug−DNA complex measured at 360 nm divided by the reduced dichroism of the same DNA sample at 260 nm in the absence of drug) with the different polymers. All four furan derivatives have negative DR values [i.e. positive reduced dichroism in complex with nucleic acids that have open minor grooves (poly $d(A-T)_2$, polydA·polydT, and poly$d(I-C)_2$] consistent with the well-characterized minor-groove binding mode of these types of structures. In contrast, all furans have positive DR values (i.e. negative reduced dichroism) with DNAs that have a wider minor groove that is blocked by the 2-NH_2 group of G [poly$d(G-C)_2$, poly(dG)·(dC), poly$d(A-G)$·$d(C-T)$, poly$d(A-C)$·$d(G-T)$] in agreement with results expected for an intercalation binding mode with the diphenylfuran aromatic system approximately parallel to the planes of the DNA base pairs. The fact that poly(dA-dC)•(dG-dT) binds DB 60 very well is plainly in agreement with the NMR data, suggesting that this compound intercalates at the ApC dinucleotide step in $d(ACGT)_2$ (see below). The natural calf thymus DNA, with mixed open and blocked minor-groove regions, generally has near zero dichroism values for the furan complexes in the

(38) Tanious, F. T.; Ding, D.; Patrick, D. A.; Titwell, R. R.; Wilson, W. D. *Biochemistry* **1997**, *36*, 15315−15325.
(39) States, D. J.; Haberkorn, R. A.; Ruben, D. J. *J. Magn. Reson.* **1982**, *48*, 286−292.
(40) Weiner, S. J.; Kollman, P. A.; Case, D. A.; Singh, U. C.; Ghio, C.; Alagona, G.; Profeta, S., Jr.; Weiner, P. *J. Am. Chem. Soc.* **1984**, *106*, 765−784.
(41) Weiner, S. J.; Kollman, P. A.; Nguyen, D. T.; Case, D. A. *J. Comput. Chem.* **1986**, *7*, 230−252.
(42) Veal, J. M.; Wilson, W. D. *J. Biomol. Struct. Dyn.* **1991**, *8*, 1119−1145.
(43) McGhee, J. D.; von Hippel, P. H. *J. Mol. Biol.* **1974**, *86*, 469−489.

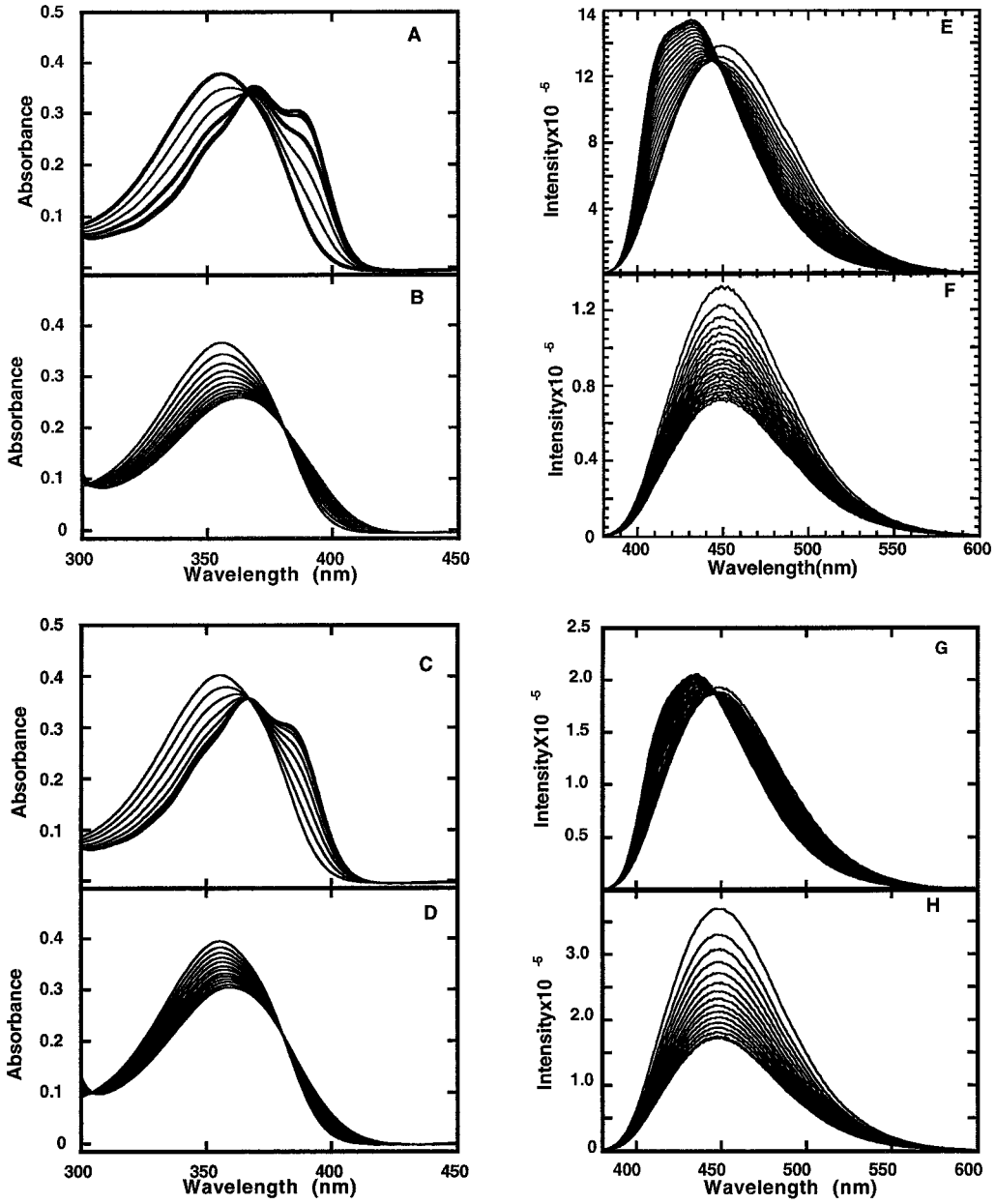

Figure 2. Spectrophotometric titrations of DB 244 (A, B), and DB 226 (C, D) with polyd(A−T)$_2$ and polyd(G−C)$_2$. Titrations were conducted in a 1 cm cell in MES buffer with 0.1 M NaCl added at 25 °C. (A) The concentrations are as follows: 1.05×10^{-5} M of DB 244, and polyd(A−T)$_2$ concentrations in base pairs of zero, 7.935×10^{-6}, 1.585×10^{-5}, 2.385×10^{-5}, 3.705×10^{-5}, 3.975×10^{-5}, 4.765×10^{-5}, 5.555×10^{-5}, and 6.345×10^{-5} respectively from the top to the bottom curves at 358 nm. (B) The concentrations are as follows: 1.05×10^{-5} M of DB 244, and polyd(C−G)$_2$ concentrations in base pairs of zero, 6.175×10^{-6}, 1.23510^{-5}, 1.855×10^{-5}, 2.465×10^{-5}, 3.085×10^{-5}, 3.705×10^{-5}, 4.325×10^{-5}, 4.935×10^{-5}, 5.555×10^{-5}, and 6.175×10^{-5} respectively from the top to the bottom curves at 358 nm. (C) The concentrations are as follows: 1.05×10^{-5} M of DB 226, and polyd(A−T)$_2$ concentrations in base pairs of zero, 7.935×10^{-6}, 1.585×10^{-5}, 2.385×10^{-5}, 3.705×10^{-5}, 3.975×10^{-5}, 4.765×10^{-5}, 5.555×10^{-5}, 6.345×10^{-5}, 7.135×10^{-5}, 7.935×10^{-5}, and 8.725×10^{-5} respectively from the top to the bottom curves at 356 nm. (D) The concentrations are as follows: 1.05×10^{-5} M of DB 226, and polyd(C−G)$_2$ concentrations in base pairs of zero, 6.175×10^{-6}, 1.235×10^{-5}, 1.855×10^{-5}, 2.465×10^{-5}, 3.085×10^{-5}, 3.705×10^{-5}, 4.325×10^{-5}, 4.935×10^{-5}, 5.555×10^{-5}, 6.175×10^{-5}, 6.785×10^{-5}, and 7.405×10^{-5} respectively from the top to the bottom curves at 356 nm. Fluorescence emission spectral titrations of DB 244 (E, F), and DB 226 (G, H) with polyd(A−T)$_2$ (E, G) and polyd(G−C)$_2$ (F, H). Titrations were conducted in a 1 cm cell with a concentration of the compounds in MES buffer with 0.1 M NaCl added at 25 °C are 3.135×10^{-7} M (E), 1.05×10^{-6} (F), 5.05×10^{-7} M (G), and 1.05×10^{-6} (H). The excitation wavelength for both compounds was 358 nm; the excitation slit was at 1 nm and the emission slit at 4 nm.

compound absorption region, as would be expected for mixed minor-groove and intercalation complexes in different sequence regions of the DNA. DB 60 has the most positive DR values of the four furans, and it is the only one of the four to have significantly negative reduced dichroism with calf thymus DNA.

Circular Dichroism Spectra. The diphenylfurans have no CD spectrum when free in solution but have induced CD spectra when complexed with nucleic acids. Unlike changes in UV−visible and fluorescence spectra, which tend to be larger for complex formation with polyd(G−C)$_2$ than with polyd(A−T)$_2$, the CD spectral changes are large with AT and very small with GC sequences (Figure 5). Consistent with the shift of the diphenylfuran absorption bands to longer wavelength on complex formation with polyd(A−T)$_2$, the furan complexes have a large induced CD peak at approximately 390 nm and a shoulder at approximately 320 nm. Significant perturbations in the AT CD bands below 300 nm are also observed. Similar induced CD spectra are observed with all of the compounds in agreement

Table 1. Binding Constants of the Furan Compounds to Polyd(A−T)$_2$ and Polyd(G−C)$_2$[a]

	$K \times 10^{-5}$	
compd	polyd(A−T)$_2$	polyd(G−C)$_2$
DB 75	190[b]	0.7[b]
DB 60	700[b]	2.3[d]
DB 244	∼1000[c]	1.14[d]
DB 226	90[c]	0.5[d]

[a] All experiments were conducted in MES buffer with 0.1 M NaCl at 25 °C. [b] Data from ref 14. [c] Binding constants were determined from fluorescence titrations, very low concentration of the compounds were used, and the data of fraction bound between 20 and 80% were used for the fit by the McGhee−von Hippel equation. [d] Binding constants were determined from UV−vis titrations (see Figure S2 in Supporting Information).

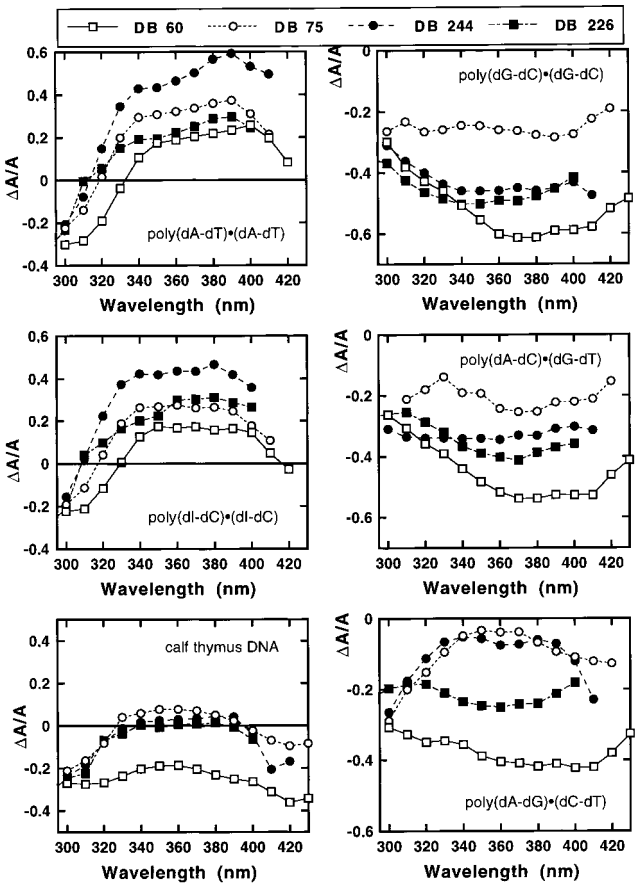

Figure 3. Reduced electric linear dichroism spectra of (open squares) DB 60, (open circles) DB 75, (closed squares) DB 226, and (closed circles) DB 244 bound to different nucleic acids. ELD spectra were obtained in the presence of 10 μM drug bound to 100 μM alternating copolymers at 13 kV/cm in 1 mM sodium cacodylate, pH 6.5.

with a similar structure for their minor-groove complexes in AT sequences. The induced CD bands for the compounds on complex formation with polyd(G−C)$_2$ are small and positive above 300 nm. All compounds cause a perturbation in the polymer structure based on the observed decrease in the DNA CD signal near 280 nm. Other regions of the polyd(G−C)$_2$ spectrum are less affected by binding of the compounds. At lower salt concentration, the compounds also give positive and slightly larger induced CD spectral changes (not shown). The spectra for all compounds are very similar in their GC complexes consistent with very similar complex structures in GC sequences.

NMR Spectra: AT Sequences. One- and two-dimensional NOESY NMR spectra were obtained for furan derivative

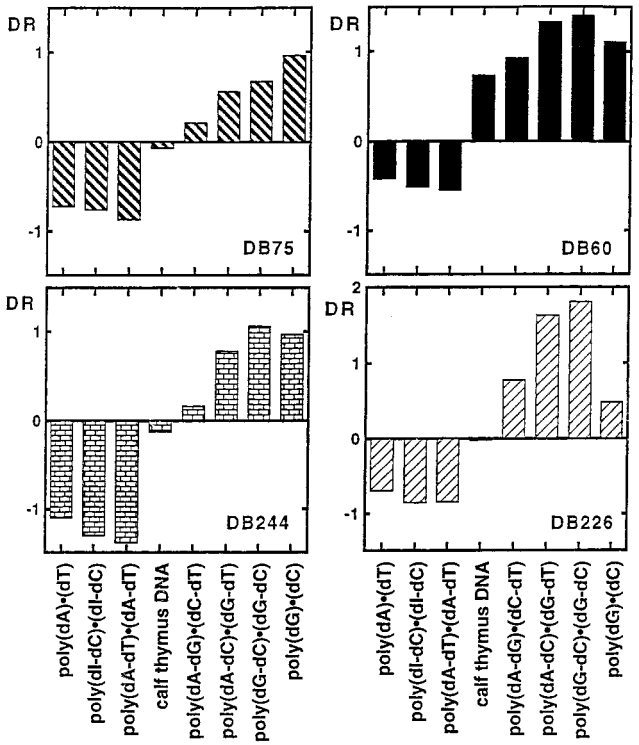

Figure 4. Variations of the dichroism ratio (DR) of the diphenylfuran derivatives bound to DNAs of different base pair composition. ELD data were recorded in 1 mM sodium cacodylate buffer, pH 6.5, at a drug/DNA ratio of 0.1 and at 13 kV/cm. ELD measurements were performed at 360 nm for the drug−DNA complex and at 260 nm for DNA alone.

complexes with the self-complementary oligomers d(A−T)$_7$, d(GCGAATTCGC), and the d(CGCGAATTCGCG) dodecamer with which several diphenylfurans have been crystallized. The latter two duplexes were studied at a level of one compound per duplex. Similar and small spectral shifts for the phenyl and furan protons were obtained in all of the d(A−T)$_7$ complexes (not shown). Spectral regions from 2D NOESY experiments are shown for DB 244, DB 226, and DB 60 in complex (1:1 ratio) with the decamer duplex to illustrate the results (Figure 6). Compound−DNA cross-peaks, such as those shown in Figure 6, involve only DNA minor-groove protons in the central AT sequence in agreement with the X-ray structures.[3,29] The DNA chemical shift changes are larger in the AT than in the GC sequence region and are similar to those observed for other minor-groove binding agents. The compound chemical-shift changes on complex formation with both the 10mer and 12mer are small and downfield as expected for minor-groove binding (Table 2). In summary, all NMR results for the compounds bound at AT sequences are consistent with the expected minor-groove complex formation.

NMR Spectra: GC Sequences. NMR spectra of all four diphenylfurans (Figure 1) have been obtained with the self-complementary oligomer d(G−C)$_7$. Spectra are shown for the DB 60 and DB 75 complexes with d(G−C)$_7$ in Figure 7A,B, and spectra for the complexes with the other furan derivatives (DB 244 and DB 226) are shown in Figure S3 (Supporting Information). Chemical shift changes on binding of all furans are collected in Table 2. For all compounds large upfield shifts of the furan and phenyl protons are observed on complex formation with the GC sequences. To obtain as much structural information on the complexes as possible, both 1D and 2D spectra of DB 60, the best intercalator of the compounds of Figure 1, complexed with the oligomer duplex tetramers

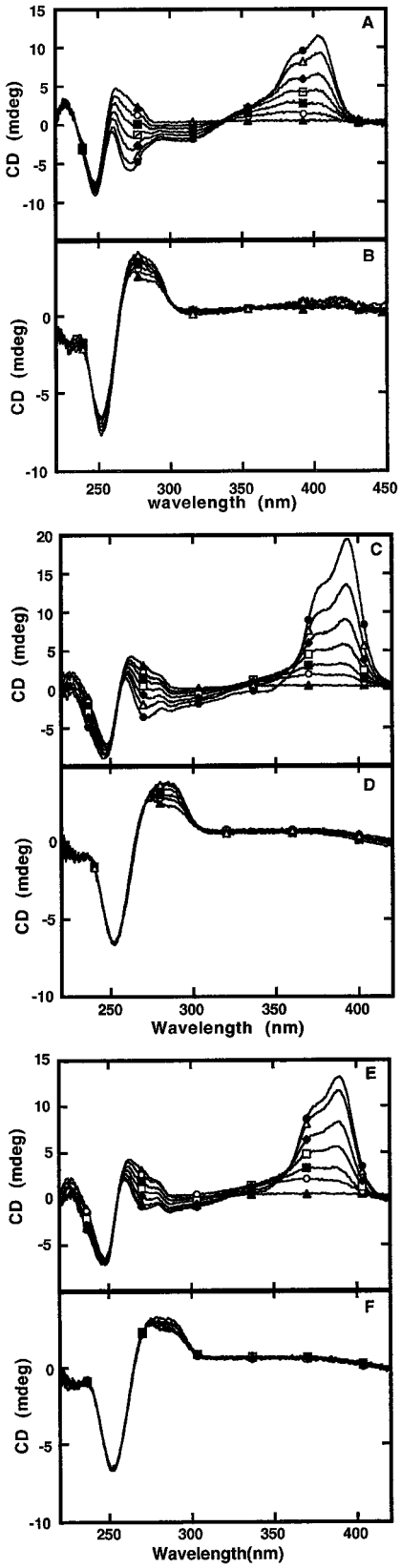

Figure 5. CD spectra of the furan compounds: (A) DB 60 with polyd(A−T)$_2$, (B) DB 60 with polyd(G−C)$_2$, (C) DB 244 with polyd(A−T)$_2$, (D) DB 244 with polyd(G−C)$_2$, (E) DB 226 with polyd(A−T)$_2$, and (F) DB 226 with polyd(G−C)$_2$. Experiments were conducted in a 1 cm cell in MES buffer with 0.1 M NaCl added at 25 °C at a polymer concentration of 2.325×10^{-5} M in base pairs. The ratio of compound/polyd(A−T)$_2$ in base pairs is 0 (▲), 0.05 (○), 0.10 (■), 0.15 (□), 0.20 (♦), 0.25 (Δ), and 0.3 (●). The ratio of compound/polyd(G−C)$_2$ in base pairs 0 (▲), 0.10 (○), 0.20 (■), 0.30 (□), 0.40 (♦), and 0.50 (△).

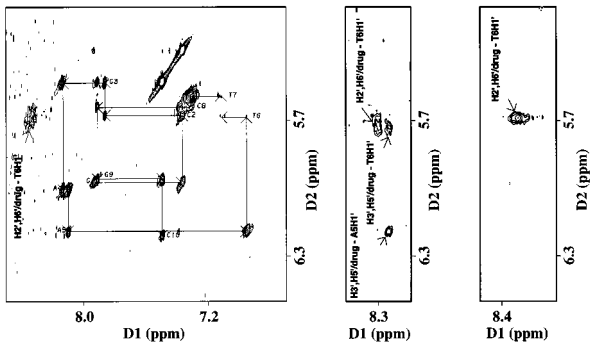

Figure 6. Expanded aromatic proton to H1′ 2D NOESY spectra are shown for DB 244, DB 60, and DB 226 respectively from the left to the right at a 1:1 ratio with d(GCGAATTCGC)$_2$. Compound−DNA cross-peaks, such those in the figure, involve only DNA minor groove protons in the central AATT region.

d(GCGC), d(CGCG), and d(ACGT) have been obtained (Figures 7C, 8). In all of these complexes, where minor-groove complex formation is inhibited, the chemical shift changes for the compound phenyl and furan proton signals are also large and upfield (Table 2), very different from the chemical shift changes observed in the AT complexes described above and strongly in support of stacking of the diphenylfuran aromatic system with the GC base pairs in an intercalation complex. We have also obtained spectra of the complex with d(CGCGAATTCGCG) at ratios greater than one compound per duplex, and as with the tetramers the diphenylfuran aromatic protons shift strongly upfield in contrast to results described above for the 1:1 complex. Results for all complexes are reported under conditions where the complexes are in fast exchange. Under these conditions only a single set of signals are observed for the phenyl 2′,6′ and 3′,5′ protons in DB 60 (Table 2). In general, at low-temperature broadening of the signals was observed, consistent with intermediate exchange kinetics, but it was not possible to obtain slow exchange conditions for any of the GC complexes.

Previous results for complexes of DB 60 and DB 75 with sonicated polyd(G−C)$_2$ are included in Table 2 for comparison with the oligomer results. Chemical shift changes for the phenyl and furan protons are similar in both the d(G−C)$_7$ and polyd(G−C)$_2$ complexes (Table 2), but much sharper spectra are obtained with the oligomer duplex at low temperature. A set of spectra at different temperatures for DB 60 and DB 75 complexed to the duplex d(G−C)$_7$ is shown in Figure 7A,B and for the other furan derivatives in Figure S3 (Supporting Information). The furan and phenyl proton signals when complexed to d(G−C)$_7$ were assigned by combination of NOESY and COSY 2D spectra (Figure S4, Supporting Information). The large upfield shifts for the phenyl and furan proton signals are maintained at high temperature (the duplex Tm is greater than 90 °C under these conditions). The compound proton signals sharpen and move slightly downfield as the temperature is increased, consistent with increased motion and some dissociation of the complex at high temperature. In summary, the chemical shift changes for all of the unfused aromatic compounds in complex with d(G−C)$_7$ or with polyd(G−C)$_2$ strongly support an intercalation binding mode.

One-dimensional NMR spectra of a 1:1 complex of DB 60 with the d(GCGC) duplex are shown at several temperatures in Figure 7C. As with the longer GC samples, large upfield shifts are obtained for the phenyl and furan protons on complex formation (Figure 7C and Table 2). NOESY spectra for the complex were obtained at several temperatures, but overlap of the GH8 signals near 7.9 ppm and of the phenyl proton and

Table 2. Chemical Shift (ppm) of the Furan (H3,4) and Phenyl Protons (H2′,6′ and H3′,5′) of the Compounds from Figure 1 in the Presence of Different DNA Samples[a]

			10mer		12mer			polyd(G−C)$_2$	d(G−C)$_7$	d(GCGC)	d(CGCG)	d(ACGT)$_2$
compd	proton	free	$R = 1.0$	$R = 2.0$	$R = 1.0$	$R = 2.0$	$R = 3.0$	($r = 0.3$)	($r = 0.5$)	($R = 1.0$)	($R = 1.0$)	($R = 1.0$)
DB244	H3,4	7.19	7.35						6.65			
	H2′,6′	8.02	8.33						7.47			
	H3′,5′	7.79	8.21						7.55			
DB226	H3,4	7.29	7.38						6.72			
	H2′,6′	8.11	8.33						7.52			
	H3′,5′	7.89	8.23						7.60			
DB60	H3,4	7.20	7.35	7.23	7.37	7.07	6.92	6.42	6.56	6.69	6.61	6.67
	H2′,6′	8.00	8.31	∼8.14	8.32	∼7.94	∼7.75	7.22	7.33	7.43	7.37	7.33
	H3′,5′	7.85	8.26	∼8.14	8.29	∼7.94	∼7.75	7.35	7.46	7.46	7.46	7.42
DB75	H3,4	7.24						6.34	6.52			
	H2′,6′	8.08						7.27	7.41			
	H3′,5′	7.91						7.40	7.51			

[a] *r*, ratio of drug to DNA base pairs; *R*, ratio of drug DNA duplex. Spectra were collected at the following temperatures: free compounds, 25 °C; 10 mer and 12 mer, 50−55 °C; d(GC)$_7$, 75 °C; tetramers, 20 °C. 10mer = d(GCGAATTCGC), and 12mer = d(CGCGAATTCGCG). Results for polyd(G−C)$_2$ are from ref 14.

C2H6 signals near 7.4 ppm (Figure 7B) prevented clear interpretation of the observed cross-peaks.

The spectral resolution is better for the 1:1 complex of DB 60 with d(CGCG), and a NOESY spectrum for that complex is shown in Figure 8A along with a summary of the compound to DNA cross-peaks. Besides the strong upfield shifts of the diphenylfuran system on complex formation, there are two very important observations from this spectrum. First, the sequential connectivity along the duplex backbone is broken or is very weak at the C1H1′ → G2H8 and C3H1′ → G4H8 steps, whereas the G2H1′ → C3H6 cross-peak is strong. Second, cross-peaks are observed from phenyl protons of the diphenyl furan ring system to DNA protons in both the major and minor grooves (for example, C1H5 and G4H1′ in Figure 8A). The first observation is consistent with an extension of the duplex at the CG steps consistent with opening of an intercalation site for the diphenylfuran ring system at the CG sites in the duplex. The second observation indicates that the diphenylfuran system must extend to both sides of the duplex, again as expected for an intercalation but not for a groove-binding mode. At a 2:1 compound-to-duplex ratio all cross-peaks between the G2H8 and C1H2′ or -2″ and between G4H8 and C3H2′ or -2″ disappear, again consistent with intercalation at the CG sites. The ^{31}P signal band for the oligomer shifts downfield approximately 0.2 ppm consistent with intercalation of the diphenylfuran aromatic system.[44]

The DB 60 complex with d(ACGT) also gives spectra with well-resolved signals, and again large upfield shifts for the DB 60 aromatic protons are observed. As with the d(CGCG) complex, cross-peaks are observed from the diphenylfuran aromatic system to protons of the d(ACGT) duplex in both the major and minor grooves. In Figure 8B the aromatic to the sugar H2′/H2″ and TCH3 chemical shift region of a 2D NOESY spectrum is shown, and cross-peaks from TCH3, AH2′/2″ and TH2′/2″ protons to the phenyl H2′,H6′ protons are observed. Cross-peaks are also observed from AH1′ and GH1′ protons to the phenyl H2′,H6′ protons in the aromatic to H1′ spectral region (not shown). All of these cross-peaks taken together suggest that the compound intercalates preferentially at the A−C/G−T positions in the d(ACGT) duplex. In summary, the 2D NOESY results with the tetramer duplexes strongly support an intercalation binding mode for the diphenylfuran derivatives.

An extremely important question is what happens in a DNA sequence that contains both potential AT minor groove binding sites as well as GC binding regions. To begin to answer this question, we have looked at the decamer and dodecamer 1:1 minor-groove complexes described above (Figure 6) at higher ratios. The furan and both sets of phenyl protons shift downfield at the 1:1 ratio, but at 2:1 and 3:1 (compound-to-duplex ratio) the shifts are reversed and move upfield, exactly as expected for the switch from groove binding to intercalation (Table 2). The chemical shift changes on complex formation for the base H8 and H6 protons are largest for AT base pairs between ratios of zero and one while the largest changes for the GC base pairs occur above a ratio of one (not shown). At the 3:1 ratio base pair connectivities along the duplex (e.g. imino to imino) are strong from base pairs 2−11 but are weak from C1−G2 and C11−G12. These latter connectivities are strong at the 1:1 ratio, and these results again support minor-groove binding at the 1:1 ratio with intercalation at the C1−G2 and C11−G12 positions as the ratio is increased. The upfield shifts are much smaller for the decamer as the ratio of compound to duplex is raised, and it appears much harder for the compound to intercalate in the three base pair sites available in the decamer. Clearly intercalation of these dications cannot occur in the immediate vicinity of the groove bound dication.

Binding Kinetics. Spectral changes observed on binding of the furan derivatives to polyd(A−T)$_2$ and polyd(G−C)$_2$ polymers were used to monitor the kinetics of binding. A plot of absorbance spectral changes as a function of time for dissociation of the furan DB 244 from polyd(A−T)$_2$ is shown in Figure 9A for illustration. Two exponential fits to the data are also shown along with plots of residuals. Dissociation rate constants were measured as a function of salt concentration at constant temperature, and plots of log(k_{app}) as a function of −log[Na$^+$] are shown in Figure 9B for DB 60, DB 75, and DB 244. For the SDS driven dissociation of these compounds from polyd(G−C)$_2$ a slope of 0.7 ± 0.1 is obtained, similar to the slope for the dicationic intercalator propidium.[33] A quite different slope of 1.7 ± 0.1 is obtained with polyd(A−T)$_2$, similar to the slope obtained for minor-groove binding compounds with polyd(A−T)$_2$.[33]

Discussion

Unfused Aromatic Cations. Interactions of unfused aromatic cations such as those shown in Figure 1 with nucleic acids are of interest for two primary reasons: they have shown very significant antimicrobial activity that appears to be related to their ability to complex with DNA,[1−9] and they provide unique probes of nucleic acid sequence-dependent molecular recogni-

(44) Gorenstein, D. G. In *Phosphorus-31 NMR: Principles and Applications*; Academic Press: Orlando, FL, 1984.

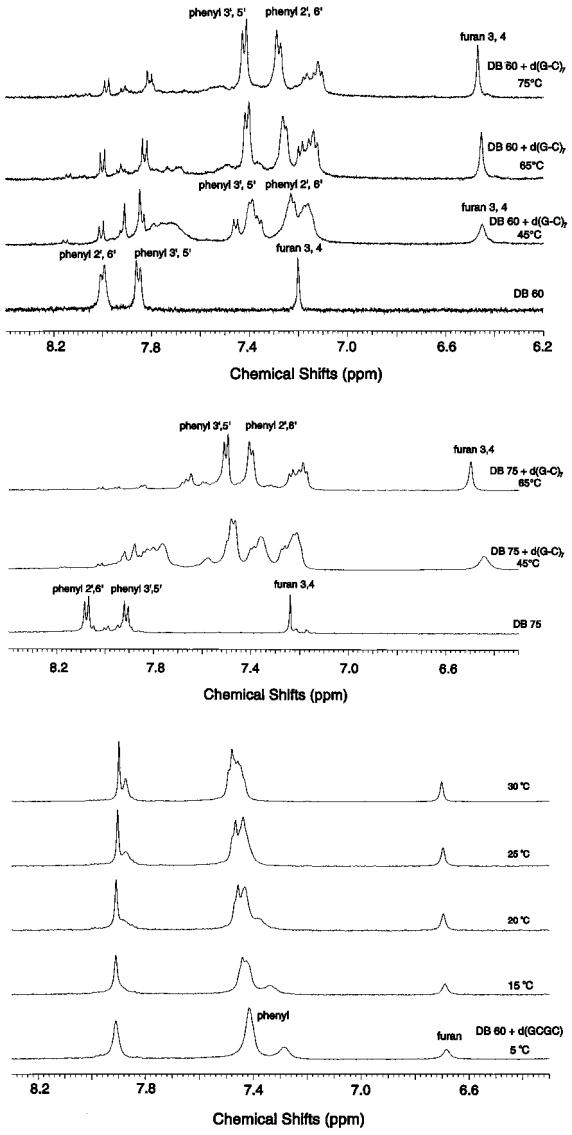

Figure 7. (A, top scale) Proton NMR spectrum of the aromatic region of DB 60 with the oligomer $d(G-C)_7$ at different temperatures. The concentration of the compound was 0.4 mM and the ratio of the compound to DNA base pairs was 0.5. (B, middle scale) Proton NMR spectrum of the aromatic region of DB 75 with the oligomer $d(G-C)_7$ at different temperatures The concentration of the compound was 0.4 mM, and the ratio of the compound to DNA base pairs was 0.5. (C, bottom scale) Proton NMR spectrum of the aromatic region of DB 60 with the oligomer d(GCGC) at different temperatures. The concentration of the compound was 1 mM, and the ratio of the compound to DNA duplex was 1.0.

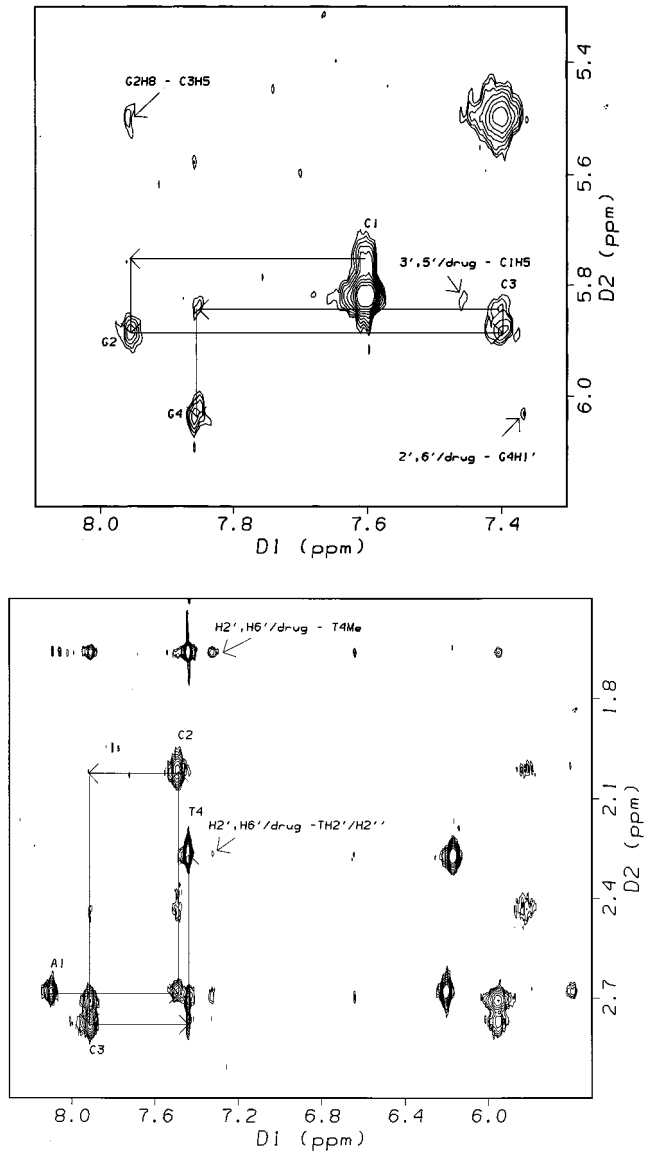

Figure 8. (A, top) Expanded aromatic proton to H1′ 2D NOESY spectrum for DB 60 in 1:1 ratio complex with oligomer d(CGCG). (B, bottom) Expanded aromatic proton H1′ 2D NOESY spectrum for DB 60 in 1:1 ratio complex with oligomer d(ACGT)

tion. The strong minor-groove-binder DB 244 shows excellent activity against *Pneumocystis carinii pneumonia* (PCP) in the immunosupressed rat model; in fact it is approximately 100 times more effective than pentamidine in this animal model. The close analogue DB 226 which binds significantly more weakly to DNA (Table 1) is much less active against PCP in the same model.[4] Interestingly, DB 244 shows in vitro activity against *Cryptococcus neoformans* near the effective dosage of fluconazole, whereas DB 226 is less effective. Unlike fluconazole, DB 244 and related furans are fungicidal.[5]

Binding Mode in AT Sequences. The mode of binding of diphenylfuran derivatives, such as those in Figure 1, in AT sequences of DNA has been investigated previously by an array of solution techniques[14,27] and by X-ray crystallography.[3,29] The conclusion from these studies, which is supported by all of the experimental results reported here, is that the compounds bind in the narrow minor groove at AT sequences with the amidines pointed to the floor of the groove for hydrogen-bond formation with acceptors on the AT base pairs. The spectral changes, for example, in the CD spectra obtained for complexes with polyd$(A-T)_2$ (Figure 5) are quite similar to those obtained for other compounds that are known to bind in the DNA minor groove at AT sites. ELD results (Figures 3 and 4) are incompatible with an intercalation binding mode but support formation of a minor-groove complex. The NMR results at 1:1 ratio for DNA sequences with four or more consecutive AT base pairs (Figure 6, Table 2) as well as the large slope obtained in plots of log k_d versus $-\log[Na^+]$ also indicate that all compounds of Figure 1 bind in the minor groove in AT sequences in a manner very similar to classical groove-binding agents such as netropsin.

The affinities of the compounds are dependent on the amidine modification, however, with DB 244, the cyclopentyl derivative, binding most strongly to AT sites, while the 3-pentyl derivative DB 226 binds most weakly. Apparent steric clash of the 3-pentyl groups with the narrow minor groove in AT sequences

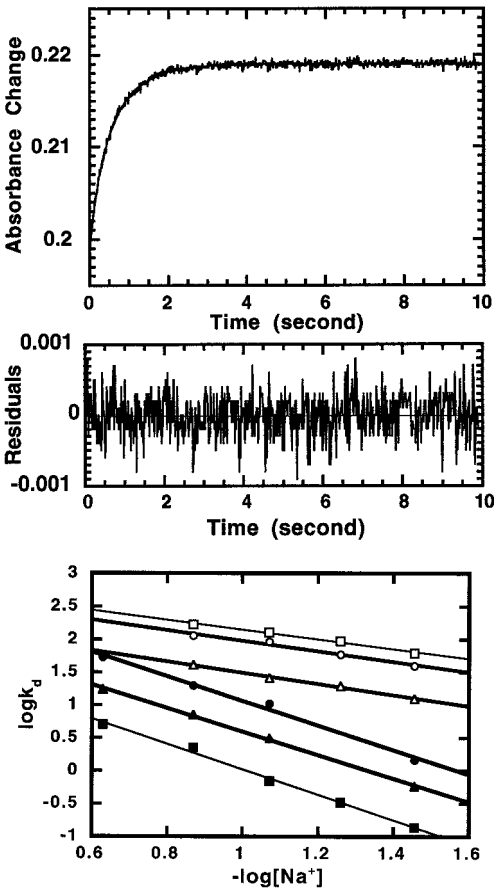

Figure 9. (A, top two plots) Stopped-flow kinetics traces for the SDS-driven dissociation of DB 244 with polyd(A−T)$_2$. The experiments were conducted at 20 °C in MES buffer with [Na^+] = 0.135 M at a ratio of 1:10 compound to polymer base pairs. The concentration of compound DB 244 after mixing was 1.05×10^{-6} M. The smooth lines in the panels are the two exponential fits to the experimental data. Residual plots are shown under the experimental plot. (B, bottom plot) Plots of log k_{app} vs −log[Na^+] for dissociation of DB 244 from poly[d(A−T)]$_2$ (■), from polyd(G−C)$_2$ (□), DB 75 from poly[d(A−T)]$_2$ (●) and from poly[d(G−C)]$_2$ (▲), and DB 60 from poly[d(A−T)]$_2$ (Δ) and from poly-[d(G−C)]$_2$ (○). Experiments were conducted in MES buffer at different ionic strengths in the manner described in A.

restricts movement of the alkyl groups on complex formation and significantly reduces the affinity of DB 226. The inescapable conclusion from this data set and results in the literature is that diphenylfurans with significantly different phenylamidine-related substituents are able to bind in the minor groove in AT sequences in a manner very similar to classical groove-binding agents.

Binding Mode at GC and mixed AT/GC Sites. Absorption, fluorescence, electric linear dichroism, CD, and NMR spectral results (Figures 2−8) as well as kinetics studies (Figure 9) clearly show that the compounds of Figure 1 form very different complexes with AT and GC sequences in DNA. The different binding modes in the different DNA sequences is not surprising since the minor groove at GC rich sequences is wider, more sterically blocked, and less electronegative than the groove in sequences of AT base pairs.[45,46] As described in the Introduction, on the basis of available experimental results, there is disagreement about how compounds related to DB 75 bind to GC and mixed sequences of DNA—arguments have been presented for intercalation[14] and for a major-groove binding mode.[26] To resolve this issue, the experiments reported here were designed to investigate the binding modes of the compounds of Figure 1 by a variety of quite different techniques. The design rationale for the compounds in Figure 1 is presented in the Introduction.

Analysis of the results presented in this paper strongly supports an intercalation binding mode for the compounds of Figure 1 in GC and mixed GC/AT sequence of DNA. The weak induced CD signals for the compounds in complex with polyd(G−C)$_2$ (Figure 5) are characteristic of intercalation, not groove binding. As can be seen from the CD patterns of these compounds in complex with polyd(A−T)$_2$, groove-binding interactions result in strong induced CD signals. The electric linear dichroism spectra with GC complexes demonstrate clearly that the compounds have their transition dipoles oriented in the same plane as the DNA base pairs, exactly as predicted for intercalation binding, and very different from the results predicted for major-groove binding (Figure 3). In addition, the results with different DNA sequences show a switch from groove binding to intercalation when the DNA minor groove has a significant number of 2-NH2 groups from GC base pairs and no continuous AT sequence (Figure 4).

The mechanisms and interaction kinetics for groove binding and intercalation of unfused aromatic cations are generally quite different. Groove-binding agents are able to bind into an existing receptor site in AT sequences of DNA, while intercalation requires opening of a space between base pairs to create a binding site. These differences result in a different influence of salt concentration on the rate constants for groove binding and intercalation. The slopes for log k_{app} versus −log[Na^+] plots, for example, are predicted to be >1.5 for groove binding and approximately half that value for intercalation. The results for AT binding of the compounds of Figure 1 are as expected for minor-groove complex formation, while the GC results are as predicted for an intercalation binding mode[33] (Figure 9).

Chemical shift changes of the aromatic proton signals of the diphenylfuran ring system of the compounds of Figure 1 are all upfield by ∼0.5 ppm or more on complex formation with GC sequences, exactly as predicted for intercalation (Figures 7 and S3). The similarity of the upfield shifts for all of the furan compounds on complex formation with the GC DNAs strongly suggests that they form very similar intercalation complexes in GC rich sequences. In addition, we have been able to obtain several useful intermolecular NOESY cross-peaks in the compound complexes with DNA tetramers, and these have been crucial in constructing molecular models for the intercalation complex of the compounds with DNA. Of particular importance is the observation that the compounds have NOE contacts to DNA protons in both the major and the minor grooves. This is only possible if the compounds extend through the DNA double helix, exactly as expected for an intercalation binding mode. Such contacts are clearly impossible for a major-groove binding mode as has been suggested for DB 75 in GC sequence.[26]

A molecular model of the complex of DB 60, based on NOE contacts with the sequence d(CGCG), was prepared by docking the compound into a CG intercalation site (Figure 10) that we have described previously.[42] All proton−proton contacts found in the NOESY experiment are within 4 Å in the model and would give the predicted NOESY cross-peaks. Much better overlap of the diphenylfuran aromatic system was obtained on

(45) Saenger, W. In *Principles of Nucleic Acid Structure*; Cantor, C. R., Ed.; Springer-Verlag: New York, 1984; pp 220−282.
(46) Kopka, M. L.; Larsen, T. A. In *Nucleic Acid Targeted Drug Design*; Propst, C. L., Perun, T. J., Eds.; Marcel Dekker: New York, 1992; pp 303−374.

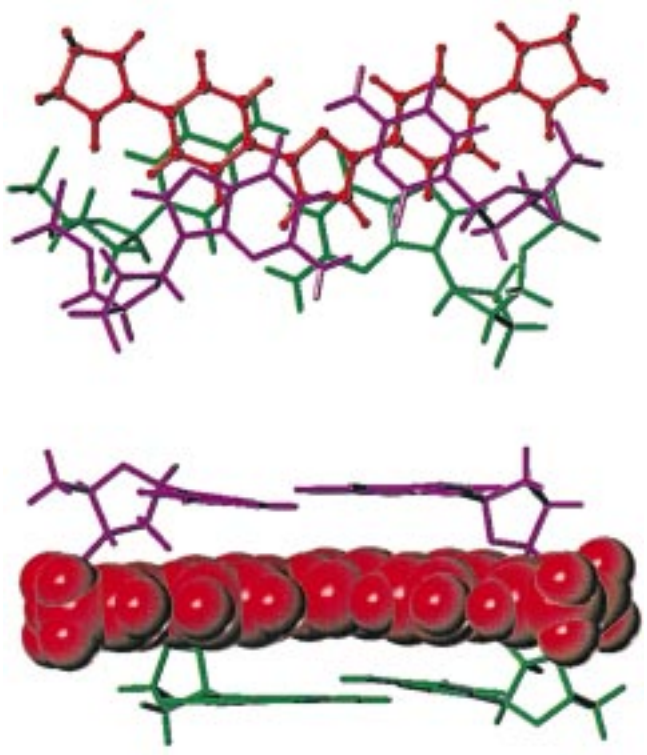

Figure 10. Views of DB 60 docked into a CG intercalation site with the imidazoline groups pointed into the major groove. (Top) A view down the helix axis onto the CG site is shown. The top base pair is purple, the bottom is green, and DB 60 is shown in red as a ball-and-stick representation. The major groove is at the top of the diagram, and the imidazoline groups can be seen at the outer edges of the site. Each imidazoline has an NH pointed directly at a nonbridging P−O group at the intercalation site. (Bottom) A view looking into the intercalation site from the major groove is shown. The base pairs are colored as in the top diagram, and DB 60 is shown in red as a space filling model. The modeling and graphics are from SYBYL 6.4 with the intercalation site and methods as previously described.[42]

docking with the imidazoline groups pointed into the major groove. In this orientation there is an additional favorable interaction through hydrogen bonds between imidazoline NH and nonbonding P−O groups on both sides of the intercalation site. Similar interactions in a minor groove complex or in a threading intercalation model, in which one imidazoline is in each groove, are not possible. Ab initio calculations indicate that the low-energy conformation of the cyclic imidazoline group is in the same plane as the diphenylfuran aromatic system (Figure 10). All of the amidine derivatives of Figure 1, however, are twisted 30−40° with respect to the diphenylfuran plane, and both stacking and possible H-bond interactions, as shown in Figure 10 for DB 60, are considerably weakened with the amidine derivatives. These observations fit all of our results, indicating that DB 60 is the strongest binding compound in non-AT sequences but is not the strongest binding compound in the AT minor-groove binding mode. The intercalation model thus provides a molecular explanation for our observations of a switch in relative binding affinity of the diphenylfuran derivatives in Figure 1 in moving from AT to GC DNA sequences and again strongly supports an intercalation binding mode in GC and mixed sequences. The prediction of a major groove complex for the compounds in GC sequences is clearly not supported by these results.

Additional strong support for an intercalation binding mode in non-AT sequences for unfused aromatic cations, such as those in Figure 1, comes from analysis of their interactions with RNA duplexes. We have shown that DB 60, for example, binds strongly to RNA, and similar results with the related diamidine berenil have been reported by Breslauer and co-workers.[23] The spectral properties of the compounds bound to RNA duplexes are very similar to their spectra with GC and mixed sequences of DNA. The duplex grooves of A-form RNA are very different from those of B-form DNA duplexes, and it is very unlikely that compounds such as DB 60 and berenil would bind strongly and with similar spectral properties to both DNA and RNA grooves. This argument is supported by the fact that classical DNA minor-groove-binding agents such as netropsin and distamycin, which cannot intercalate, bind to RNA very weakly.[18] On the other hand, the intercalation sites in DNA and RNA are quite similar, and standard intercalators such as proflavine and ethidium bind very well to DNA and RNA.[19,47] Detailed studies of the RNA complexes of unfused aromatic cations have provided strong evidence to confirm an intercalation binding mode with RNA duplexes. Again, both molecular structural logic as well as considerable experimental evidence indicate an intercalation binding mode for unfused aromatic cations in GC and mixed sequences of DNA and with RNA.

With the firm establishment of a minor-groove binding mode for the compounds of Figure 1 at AT sites and an intercalation binding mode at GC and mixed AT/ GC sequences, it is important to ask why atomic force microscopy and flow linear dichroism studies lead to erroneous conclusions for these compounds. The microscopy uses specific length DNA from plasmids of heterogeneous DNA. Our dichroism results with calf thymus DNA indicate mixed-groove-binding and intercalation interactions, as expected for a heterogeneous sequence, and no significant dichroism can be observed in this situation (Figure 4). Some localized bending of the DNA binding site on complex formation with the unfused aromatic system may also contribute to the failure of the microscopy method to detect the intercalation binding mode. Heterogeneous sequence natural DNA samples have fewer sequences of four or more AT base pairs, as required for minor-groove complex formation, but these sequences have a higher binding constant for the compounds than the more prevalent GC and mixed sequence DNA intercalation sites, and a mix of binding modes is obtained. The oligomer NMR studies with the 10mer and 12mer (Table 2) provide additional insight into how the unfused aromatic cations fill binding sites in heterogeneous DNA. The AATT site binds most of the compound up to the 1:1 ratio of compound to duplex. Addition of more compound results in intercalation of DB 60 in the CGCG regions of the DNA 12mer, and NMR results suggest that the compound goes to the C1−G2/G11−C12 sites, as far from the groove-bound species as possible. This site is removed from the 10mer and intercalation is much weaker in the 10mer than in the 12mer. These results suggest that in heterogeneous DNA minor-groove binding significantly inhibits intercalation in sites up to at least one turn of the DNA helix. This could be due to a combination of electrostatic repulsion between the groove-bound and intercalated dications and local conformational perturbations of the duplex by the groove-bound species that inhibit intercalation.

The flow linear dichroism results of DB 75 in complex with polyd$(G-C)_2$[26] cannot be explained by mixed binding modes. In the long-wavelength region, where there is only one transition (polarized along the long axis of the diphenylfuran aromatic system), flow dichroism results indicate that the transition dipole is in the plane of the DNA base pairs, exactly as predicted for

(47) Bailly, C.; Colson, P.; Houssier, C.; Hamy, F. *Nucleic Acids Res.* **1996**, *24*, 1460−1464.

an intercalation complex and in agreement with all of our results. In the lower wavelength regions (between 300 and 340 nm), the signal-to-noise drops and there are overlapping transitions, including a transition polarized along the molecular short axis of the diphenylfuran aromatic system. The reduced dichroism results in this region have been used to predict a major groove complex for DB 75. All results can be reconciled, however, if the low-wavelength results are complicated by the low *S/N* as well as the overlapping transitions that can confuse interpretations of the dichroism results in this region. Variations in flow linear dichroism with wavelength, similar to those observed for the DB 75 complex, have recently been reported for a fused ring aromatic intercalator[48] and illustrate some of the problems in interpretation of changes in dichroism amplitude in terms of changes in binding mode. The microscopy and flow dichroism results may supply some very important information about the structure of the intercalation site for unfused aromatic compounds, particularly if the experiments are conducted with homopolymers, but under the conditions used, these two experiments do not provide a challenge to the overwhelming evidence in support of an intercalation binding mode.

(48) Becker, H.-C.; Norden, B *J. Am. Chem. Soc.* **1997**, *119*, 5798−5803.

Acknowledgment. This work was done under the support of NIH research Grants AI-33363 and AI-39391 (to W.D.W and D.W.B.) and from the Ligue Nationale Frangaise Contre le Cancer (Commité du Nord) (to C.B). Support by the "Convention INSERM-CFB" is acknowledged.

Supporting Information Available: UV−vis spectra of furan derivatives of Figure 1, Scatchard plots of DB 60 binding to polyd(G-C)$_2$, ^{1}H NMR spectra of DB 226 and DB 244 with d(G-C)$_7$, and 2D COSY and NOESY NMR spectra of DB 60 with d(G-C)$_7$ (6 pages, print/PDF). See any current masthead page for ordering information and Web access instructions.

JA981212N